Vietnam Journal of Science and Technology ***57*** *(6) (2019) 773-787*

doi:10.15625/2525-2518/57/6/13917

INVERSE DYNAMIC ANALYSIS OF MILLING MACHINING ROBOT: APPLICATION IN CALIBRATION OF CUTTING FORCE

Ha Thanh Hai[1, 2]

[1]*Hanoi University of Science and Technology, No1, Dai Co Viet St, Hai Ba Trung, Ha Noi*

[2]*College of Urban Works Construction, Yen Thuong, Gia Lam, Ha Noi*

Email: *hathanhhai1976@gmail.com*

Received: 7 July 2019; Accepted for publication: 8 August 2019

Abstract. This article presents analysis of inverse dynamics of a serial manipulator in milling process. With the exception of positioning accuracy issue, machining by robots have more advantages than by conventional CNC milling machines, due to higher flexible kinematics (many links and degrees of freedom) and larger working space. Therefore, motion of the robot links is more complicated. Process forces and complicated motion involve to difficulties in solving dynamic problems of robots. This affects the robot control to match machining requirements. This article utilizes the transformation coordinates and the homogeneous transformation matrices to analysis of kinematics and dynamics of the robot. In general, cutting forces are determined by using empirical formulas that lead to errors of cutting force values. Moreover, the cutting forces are changing and causing vibration during machining process. Errors of cutting force values affect the accuracy of the dynamic model. This paper proposes an algorithm to compute the cutting forces based on the feedback values of the robot's motion. The results of kinematic and dynamic simulation of the computing program and calibrating cutting force prove intuitively and reliably validation of the proposed method.

Keywords: machining robot, milling, dynamic analysis, cutting force, calibration.

Classification numbers: 5.3.8, 5.3.5.

1. INTRODUCTION

Because of many advantages, demands of applying robots in machining operations have been strongly increasing [1 - 5]. Thank to flexible kinematic structure with many degrees of freedom, robots are able to reach to any difficult orientation and position of an end-effector that match different technical demands. Robots are programed to perform various machining operations. These advantages enable robots to machine favourably variety of parts, from simple shapes and average accuracy to complicated shapes and high accuracy, such as polishing, grinding and de-burring, and milling.

Beside the advantages, there are difficulties and challenges that being addressed to use robots for machining tasks [2, 6]. Firstly, due to a large number of links, motion of the last link

or the end-effector is a combination motion of the privious links. To perform spatial complex motion of the end-effector, robots need to have 5 to 6 degrees of freedom, including at least 3 revolute joints to ensure the end-effector is able to reach to arbitrary orientation. Therefore, it is difficult to determine motion of the end-effector; the formulas of the angular velocity and acceleration are cumbersome. As a result, it is hard to derive and solve the complicated kinematic and dynamic equations, except that they are performed by automatic computing program.

Cutting forces are significant influential elements in the dynamic equations of the robots. The accuracy of computation process forces affects the accuracy of motion control of the robots in machining tasks. It is hard to compute precisely process force values, due to process force values denpend on materials, cutting parameters, dynamic properties of the robots. Cutting forces are often calculated by empirical formulas in engineering handbooks that lead to remarkable errors. It is able to use measuring force sensors to improve accuracy of cutting force calculation in the differential equations of motion. This approach increases complexity of the control system and product cost as well.

The serial chain and open loop structure leads to the low structural stiffness of robots that cause some deformations of robot joints and links. Especially, material heterogeneity, changes of the cutting process parameters and discontinuous cutting of cutting tooths creat frequent variations of process forces that generate chatters and errors in machining processes.

A large number of studies have been carrying out to cope with the difficulties and challenges to enable high performance of robots in machining tasks. The authors in [7] has proposed a method to design trajectories and analyze dynamics of robot in machining. The works in [8,9] present a general method to derive differential equations of motion; meanwhile, in [9], the calibration of cutting forces is briefly mentioned. The analysis of control problems and process forces of robots are investigated in [10 - 12].

This paper uses transformation coordinates and the homogeneous transformation matrices to express positions and orientations of the robot links. This enables to derive and solve automatically kinematic and dynamic equations that match favourably machining performance of the robot.

To calculate process force values in the differential equations of motion, [8,9] use the empirical formulas, cutting force values is estimated in average. However, as mentioned, the process forces vary by many causes, one of the causes is chatter or vibration, which are presented in many studies, such as the works presented in [13 - 15]. The average cutting force values that are defined by the empirical formulas exist remarkable errors. This paper presents the analysis of dynamic model that includes changing of cutting forces in machining process. Process forces are functions of time and calculated by time. In addition, although calculating by time, there are errors of cutting force values, becauce of relative accuracy of the empitical formulas. The method of computing errors to calibrate cutting forces is presented in this paper.

This paper is constructed into six parts including introduction, robot kinematics, deriving differential equations of motion, computing inverse dynamics, algorithms to calibrate cutting forces, computing illustrations and simulations.

2. ROBOT KINEMATICS

This paper investigates a model of a serial and six degrees of freedom manipulator that employs form-shaping machining of part’s surfaces. Figure 1 shows the kinematic diagram of

the robot that consists of 6 movable links connecting to a fixed base, and a clamping device which is used to clamp workpieces. The links of robot are notated LK0 (the fixed base), LK1, LK2,…, LK6 (the end-effector), respectively. B is notation of the clamping device.

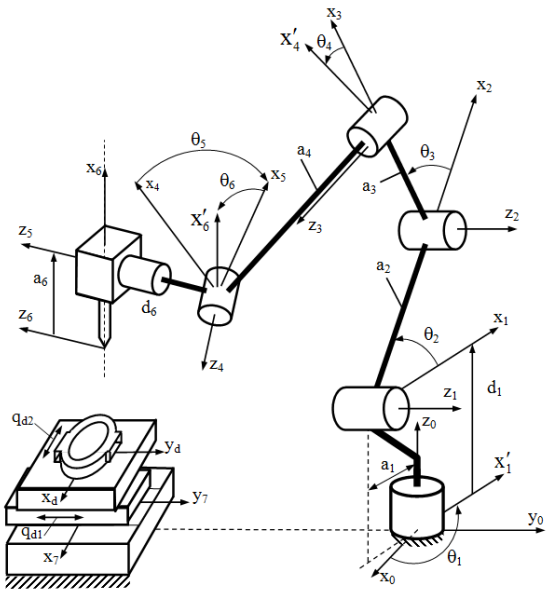

Figure 1. Kinematic diagram of the machining robot.

2.1. Kinematics of form-shaping machining of robot

According to the form-shaping theories [16], to carry out form-shaping motions, tool paths need to be determined, as path L of Figure 2. The cutter moves along the tool paths to fulfill machining tasks. Suppose that geometrical parameters of machining surfaces and tool paths are determined and expressed in a frame. This frame is often attached to its locating base, is called the workpiece frame, and notated as $O_dx_dy_dz_d$ (as shown Figure 2).

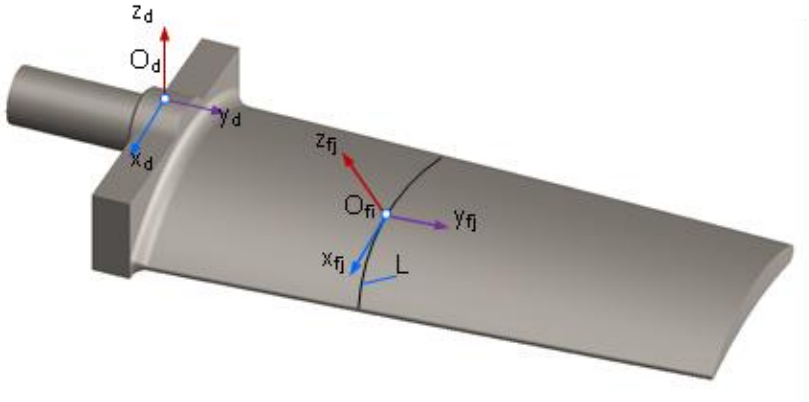

Figure 2. The workpieces, the tool path, the tool frame.

To express the tool paths in the workpiece frame, an orthonormal frame that have three orthogonal axes, called the workpiece trihedron to distinguish with the workpiece frame, denoted as $O_{fj}x_{fj}y_{fj}z_{fj}$ (Figure 2). The origin O_{fj} is located at the point j on the tool path. The

orientation of the workpiece trihedron is defined to ensure the axis x_{fj} is tangent line of the tool path, z_{fj} is normal line of the tool path, y_{fj} is chosen so as to complete a right-handed frame. Therefore, the workpiece trihedron characterizes geometrical shapes of the machining surfaces and the tool paths. Notation of position and orientation parameters of the workpiece trihedron $O_{fj}x_{fj}y_{fj}z_{fj}$ with respect to the workpiece frame are $x_j, y_j, z_j, \alpha_j, \beta_j, \eta_j$, respectively. The workpiece trihedron is represented in the workpiece frame by the homogeneous transformation matrix ${}^{d}A_{fi}$.

$$ {}^{d}p_{fi} = \left[{}^{d}x_{fi}, {}^{d}y_{fi}, {}^{d}z_{fi}, {}^{d}\alpha_{fi}, {}^{d}\beta_{fi}, {}^{d}\eta_{fi} \right]^{T} \tag{1} $$

$$ {}^{d}A_{fi}\left(q_i\right) = \begin{bmatrix} {}^{d}C_{fi}\left({}^{d}\alpha_{fi}, {}^{d}\beta_{fi}, {}^{d}\eta_{fi}\right) & {}^{d}r_{fi}\left({}^{d}x_{fi}, {}^{d}y_{fi}, {}^{d}z_{fi}\right) \\ 0^{T} & 1 \end{bmatrix} \tag{2} $$

The world frame is $O_0x_0y_0z_0$. The workpiece is located on the clamping device; the position and orientation of the workpiece frame $O_dx_dy_dz_d$ with respect to the world frame, are determined by general coordinates ${}^{0}x_d, {}^{0}y_d, {}^{0}z_d, {}^{0}\alpha_d, {}^{0}\beta_d, {}^{0}\eta_d$, and expressed by matrix ${}^{0}A_d$. Producting the both sides of (2) to ${}^{0}A_d$, we obtained the equations that express the workpiece trihedron with respect to the world frame $O_0x_0y_0z_0$.

$$ {}^{0}A_{fi}\left({}^{d}p_{fi}\right) = {}^{0}A_{d}\,{}^{d}A_{fi}\left({}^{d}p_{fi}\right) = \begin{bmatrix} {}^{0}C_{fi}\left({}^{d}\alpha_{fi}, {}^{d}\beta_{fi}, {}^{d}\eta_{fi}\right) & {}^{0}r_{fi}\left({}^{d}x_{fi}, {}^{d}y_{fi}, {}^{d}z_{fi}\right) \\ 0^{T} & 1 \end{bmatrix} \tag{3} $$

Applying the accompanying trihedron method [7, 17, 18], the cutting area on the cutter is characterized by an orthonormal frame, notated as $O_Ex_Ey_Ez_E$, called the tool trihedron or the tool frame. Notation of position and orientation parameters of the frame $O_Ex_Ey_Ez_E$ with respect to the workpiece frame are ${}^{d}x_E, {}^{d}y_E, {}^{d}z_E, {}^{d}\alpha_E, {}^{d}\beta_E, {}^{d}\eta_E$, expressed by vector ${}^{d}p_E$. The expression of the tool trihedron with respect to the workpiece frame is the homogeneous transformation matrix ${}^{d}A_E$.

$$ {}^{d}p_{E} = \left[{}^{d}x_{E}, {}^{d}y_{E}, {}^{d}z_{E}, {}^{d}\alpha_{E}, {}^{d}\beta_{E}, {}^{d}\eta_{E} \right]^{T} \tag{4} $$

$$ {}^{d}A_{E}\left(q_i\right) = \begin{bmatrix} {}^{d}C_{E}\left({}^{d}\alpha_{E}, {}^{d}\beta_{E}, {}^{d}\eta_{E}\right) & {}^{d}r_{E}\left({}^{d}x_{E}, {}^{d}y_{E}, {}^{d}z_{E}\right) \\ 0^{T} & 1 \end{bmatrix} \tag{5} $$

The expression of the tool trihedron with respect to the world frame is the matrix ${}^{0}A_E$.

$$ {}^{0}A_{E}\left({}^{d}p_{E}\right) = {}^{0}A_{d}\,{}^{d}A_{E}\left({}^{d}p_{E}\right) = \begin{bmatrix} {}^{0}C_{E}\left({}^{d}\alpha_{E}, {}^{d}\beta_{E}, {}^{d}\eta_{E}\right) & {}^{0}r_{E}\left({}^{d}x_{E}, {}^{d}y_{E}, {}^{d}z_{E}\right) \\ 0^{T} & 1 \end{bmatrix} \tag{6} $$

From robot kinematic point of view, the matrix of (6) expresses poses of the tool in the operational space. The components of ${}^{0}A_E$ are functions of the operational vector ${}^{d}p_E$ (4).

Depending on geometrical shapes of machining surfaces, there are requirements of relative position and orientation between the tool trihedron and the workpiece trihedron, to guarantee the tool move along the tool paths. In the case of special surface form-shaping, the two frame must coincide. Therefore, the matrix ${}^{d}A_E$ from (6) is determined by (3), we obtained:

$$ {}^{0}A_{fi}\left({}^{d}p_{E}\right) = {}^{0}A_{E}\left({}^{d}p_{fi}\right) \tag{7} $$

Using the presented frames and transformation matrices, combine with equation (7) to describle form-shaping kinematic of the robot:

- At every instant time, motion of the robot moving the cutting tool ensures that the tool trihedron matches (7).

- The velocity of the tool with respect to the machining surface is expressed by the velocity of the tool trihedron with respect to the workpiece frame.

2.2. Kinematic equations of the robot

To determine the frames and compute the homogeneous transformation matrices, Denavit-Hartenberg convention is utilized. In Figure 1, the frames are notated as $O_ix_iy_iz_i$; I = 0,1,..,6; correspoding to the links: LK0, LK1, .., LK6; in which the frame $O_0x_0y_0z_0$ is the base frame.

The frame that is attached to the end-effector, as mentioned above, is the tool trihedron $O_Ex_Ey_Ez_E$. To simplify the expressions and remain generality, the frame that attached to the clamping device is chosen as the workpiece frame when the workpiece is clamped on the clamping device, $O_dx_dy_dz_d$.

The joint coordinates are q_1, q_2,..,q_6:

$$q = \left[q_1,..,q_6\right]^T = \left[\theta_1,..,\theta_6\right]^T \tag{8}$$

The Denavit-Hartenberg homogeneous transformation matrix between the two coordinate frames of the two consecutive links (from frame i-1 to frame i) is notated by ${}^{i-1}A_i$. Therefore, ${}^{i-1}A_i$ represents position and orientation of the frame i with repect to the frame i-1, i=1,..,6. The elements of matrix ${}^{i-1}A_i$ are functions of the joint coordinate q_i.

Possition and orientation of the tool frame $O_Ex_Ey_Ez_E$ with repect to the coordinate frame of the end-effector are determined by the general coordinates ${}^6x_E$, ${}^6y_E$, ${}^6z_E$, ${}^6\alpha_E$, ${}^6\beta_E$, ${}^6\eta_E$, and represented by matrix ${}^6A_E$.

Possition and orientation of the clamping coordinate frame (the workpiece frame) $O_dx_dy_dz_d$ with repect to the world frame are determined by the general coordinates ${}^0x_d$, ${}^0y_d$, ${}^0z_d$, ${}^0\alpha_d$, ${}^0\beta_d$, ${}^0\eta_d$, and represented by the matrix ${}^0A_d$, as given above.

Considering the kinematic chain:

The world frame $\rightarrow$ the robot's link frames $\rightarrow$ the tool frame.

Applying Denavit-Hartenberg convention of homogeneous transformation matrices, we obtained the matrix ${}^0A_E(q)$, which represents the position and orientation of the tool frame with respect to the world frame.

$${}^0A_E = {}^0A_1\left(q_1\right){}^1A_2\left(q_2\right)...{}^5A_6\left(q_6\right){}^6A_E \tag{9}$$

From the robot kinematic point of view, the matrix in equation (9) represents the cutting tool's pose complying with the robot kinematical structure, and expresses in joint space.

Due to (6) and (9), we obtain kinematic equation in matrix form (10).

$${}^0A_d\,{}^dA_E\left({}^dp_E\right) = {}^0A_1\left(q_1\right){}^1A_2\left(q_2\right)...{}^5A_6\left(q_6\right){}^6A_E \tag{10}$$

The left side of (10) is a function of the operational coordinate vector ${}^dp_E$. The right side of (10) is a function of the joint coordinate vector q.

Direct kinematic problem

To determine the position and orientation of the cutting tool with respect to the workpiece that is expressed by (4), the direct kinematic problem is analyzed. The joint positions, angular

velocities, angular accelerations can be measured by sensors. Rewrite equation (10) into the following form:

$$ {}^{d}A_{E}\left({}^{d}p_{E}\right) = {}^{0}A_{d}^{-1}\,{}^{0}A_{1}\left(q_{1}\right){}^{1}A_{2}\left(q_{2}\right)...{}^{5}A_{6}\left(q_{6}\right){}^{6}A_{E} \tag{11} $$

The right side of (11) is completely determined, so that solving (11) to compute the coordinates, velocities and accelerations of the end-effector and the cutter, this is a common problem.

Inverse kinematic problem

The inverse kinematic problem is a significant problem of form-shaping machining. Demanding to determine the joint coordinates and its derivatives, or determine motion of the links to guarantee requirement of the form-shaping motion.

When analyzing inverse kinematic problem, the operational coordinates (4) that are determined by (1) has been computed. Rewrite equation (10) into the form of nonlinear algebraic equations:

$$ f\left(q,p\right) = 0 \tag{12} $$

Here, the set of the equations includes six equations:

$$ f = \left[f_{1},...,f_{6}\right]^{T} \tag{13} $$

q is the joint position vector, expessed by (8), p is the operational coordinate vector ${}^{d}p_{E}$, expessed by (4).

To solve the inverse problem of joint velocity and acceleration, it needs to determine the tool velocity along the tool path, which is determined by the requirements of form-shaping machining engineering. Suppose that from the requirements of velocity and acceleration of the tool moving along the tool path we computed derivatives of the operational coordinates (4) in (14), (15).

$$ \dot{p} = \left[{}^{d}\dot{x}_{E},\,{}^{d}\dot{y}_{E},\,{}^{d}\dot{z}_{E},\,{}^{d}\dot{\alpha}_{E},\,{}^{d}\dot{\beta}_{E},\,{}^{d}\dot{\eta}_{E}\right]^{T} \tag{14} $$

$$ \ddot{p} = \left[{}^{d}\ddot{x}_{E},\,{}^{d}\ddot{y}_{E},\,{}^{d}\ddot{z}_{E},\,{}^{d}\ddot{\alpha}_{E},\,{}^{d}\ddot{\beta}_{E},\,{}^{d}\ddot{\eta}_{E}\right]^{T} \tag{15} $$

Carring out first and second derivatives of equation (13) with respect to time t (16), (17), (18), respectively, we obtained the relative velocities and accelerations of the links (19), (20).

$$ J_{q}\dot{q} = J_{p}\dot{p} \tag{16} $$

$$ J_{q} = \frac{\partial f}{\partial q};\quad J_{p} = -\frac{\partial f}{\partial p} \tag{17} $$

$$ \dot{J}_{q}\dot{q} + J_{q}\ddot{q} = \dot{J}_{p}\dot{p} + J_{p}\ddot{p} \tag{18} $$

$$ \dot{q} = J_{q}^{-1}J_{p}\dot{p} \tag{19} $$

$$ \ddot{q} = J_{q}^{-1}\left[\dot{J}_{p}\dot{p} + J_{p}\ddot{p} - \dot{J}_{q}\dot{q}\right]. \tag{20} $$

3. DYNAMIC EQUATION OF ROBOT

The Lagrange equations of the robot in matrix form can be expressed as follows (21):

$$M(q)\ddot{q} + C(q,\dot{q}) + G(q) + Q = U \tag{21}$$

here: M(q) – is the mass matrix, which is computed as (22).

$$M(q) = \left[\sum_{i=1}^{6} \left(J_{Ti}^{T} m_i J_{Ti} + J_{Ri}^{T} {}^{ci}\Theta_{ci} J_{Ri} \right) \right]_{6\times 6} \tag{22}$$

$$J_{Ti} = \frac{\partial r_{ci}}{\partial q} \tag{23}$$

$$J_{Ri} = \frac{\partial {}^{i}\omega_i}{\partial \dot{q}} \tag{24}$$

where r_{ci} is the coordinate vector of the center of mass of link i, ${}^{i}\omega_i$ is the angular velocity of link i, expressed in the frame i [19].

In (22), m_i is the mass of link i; J_{Ti} is the translation Jacobian matrix of the coordinate vector of the center of mass of link i, expressed with respect to the joint coordinates (23); J_{Ri} is the rotation Jacobian matrix of the angular velocity vector of link i, expressed with respect to the derivatives of joint coordinates (24); ${}^{ci}\Theta_{ci}$ is the inertia tensor of link i about the center of mass C_i, expressed in the frame which is attached to C_i.

The position of the center of mass of link i, angular velocity of link i can be computed by following the kinematic problem.

$C(q,\dot{q})$ is the general force vector of coriolis and centrifugal forces (25), (26), (27).

$$C(q,\dot{q}) = [c_1, c_2, .., c_6]^T \tag{25}$$

$$c_j = \sum_{k,l=1}^{6} (k,l;j)\dot{q}_k \dot{q}_l \tag{26}$$

$$(k,l;j) = \frac{1}{2}\left(\frac{\partial m_{kj}}{\partial q_l} + \frac{\partial m_{lj}}{\partial q_k} - \frac{\partial m_{kl}}{\partial q_j} \right) \tag{27}$$

with (k,l;j) is Christofel notation.

G(q) – is the vector of general forces of the gravitational forces (28), (29).

$$G(q) = [g_1, g_2, .., g_6]^T \tag{28}$$

$$g_j = \frac{\partial \Pi}{\partial q_j} \tag{29}$$

U – is the vector of general forces of the driving forces (30), (31).

$$U = [U_1, U_2, .., U_6]^T \tag{30}$$

$$U_i = \tau_i \tag{31}$$

here, τ_i is the driving torque of joint i.

Q(q) – is the vector of general forces and torques of nonconsevertive forces, such as cutting forces, acting forces, etc. In this paper, we only consider cutting forces.

The cutting forces are determined by an empirical formula corresponding to a certain machining process. Considering a use case which is shown in Figure 3, where presents cutting

forces of an end mills in down milling process. From Figure 3, the cutting force can be expressed in the workpiece frame or in the tool frame. F_c is denoted the cutting force component, M_c is denoted the applied moment. On the other hand, from (9) we can compute the Jacobian matrices by using (32).

$$J_{Fc} = \frac{\partial r_E}{\partial q}; \quad J_{Rc} = \frac{\partial \omega_E}{\partial \dot{q}} \tag{32}$$

wwhere r_E is the locating vector of cutting point E of the tool's cutting edge, ω_E is the angular velocity of the end effector.

Thus, we can express the vector of general forces of the cutting forces in the robot differential equations of motion [19].

$$Q = J_{Fc}^T F_c + J_{Rc}^T M_c = \left[J_{Fc}^T, J_{Rc}^T \right] \begin{bmatrix} F_c \\ M_c \end{bmatrix} = JR \tag{33}$$

The cutting forces depend on some major parameters such as: depth of cut t, feed rate s, spindle speed n, width of cut B, etc. The cutting force components are not constants because the material is not homogeneous, and depth of cut, feed rate, etc can be changed on the tool path. Besides, because of the cutting tooths positioning on the tool, the cutting tooths do not cut continuously, the cutting forces are also not continuous and changing periodically which generate vibrations. For simplicity, in [8,9] we chose the average value in the inverse dynamic problem to compute the driving forces or torques of the robot.

To realize a more practical computation method, let us assume that the cutting force components consist of an average value and plus an error that is expressed by a function with respect to time. In practice, the tool has a certain number of teeth, so that the teeth cut the surface periodically, depends on the number of the teeth and spindle speed; we express the errors of the cutting forces from their average values by sin functions (34).

$$\Delta F_c = eF \sin(\Omega t); \quad \Delta M_c = eM \sin(\Omega t) \tag{34}$$

In (34), ΔF_c, ΔM_c are the deviations of cutting forces that have sin-wave forms. eF, eM – is the amplitude, which is half of the difference between the maximum and minimum values of cutting forces/moments in a cutting period, depending on the number of the tooths cutting on the surface, spindle speed, *etc*. Ω - is the frequency, which is computed in each cutting process [20,21].

The general cutting force deviation is expressed with respect to the joint coordinates as follows:

$$\Delta Q = J_{Fc}^T \Delta F_c + J_{Rc}^T \Delta M_c = \left[J_{Fc}^T, J_{Rc}^T \right] \begin{bmatrix} \Delta F_c \\ \Delta M_c \end{bmatrix} = J \Delta R \tag{35}$$

The differential equations of motion of the robot with varying cutting forces:

$$M(q)\ddot{q} + C(q,\dot{q}) + G(q) + Q + \Delta Q = U \tag{36}$$

Equation (36) gives a better dynamic analysis when we consider the variation of the cutting force in a finite value, which is assumed to be expressed in a sin function.

4. INVERSE DYNAMIC ANALYSIS

In the following, we give an example of applying the inverse dynamic model to a down

milling process by an end mill. The cutting forces diagram, the workpiece trihedron and the cutter are shown in Figure 3.

The workpiece is the middle housing of a hydraulic pump, using C40 steel, the milling surface is a plane with the tool path as shown in Figure 4.

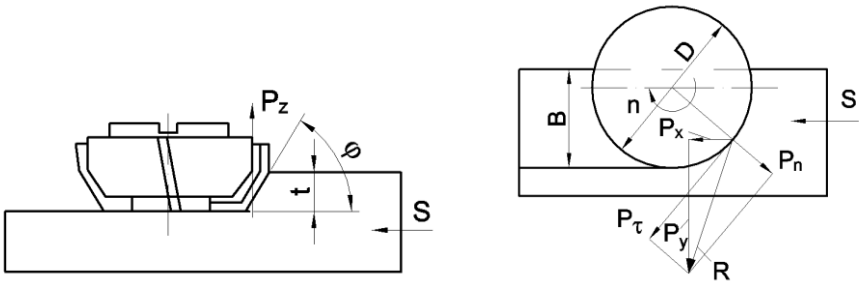

Figure 3. Representation of cutting forces.

P_τ - Tangential cutting force; P_n – radial cutting force; P_x - X-directional cutting force

P_y - Y-directional cutting force; P_z - Z-directional cutting force.

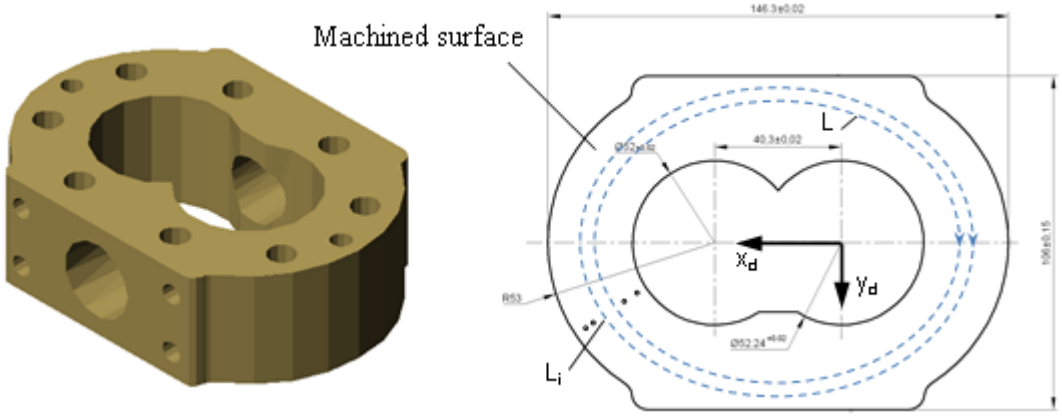

Figure 4. Workpiece, shaping path.

The robot in Figure 1 is chosen as the machining robot of The ABB - the IRB 6660 robot.

Table 1. Denavit-Hartenberg kinematic parameters of the robot.

Links	θ_i	d_i	a_i	α_i
1	θ_1	d_1	a_1	$\pi/2$
2	θ_2	*0*	a_2	*0*
3	θ_3	*0*	a_3	$-\pi/2$
4	θ_4	d_4	*0*	$\pi/2$
5	θ_5	*0*	*0*	$-\pi/2$
6	θ_6	d_6	a_6	*0*

The kinematic parameters of the robot are given in Table 1 (by using Denavit-Hartenberg convention).

The geometric parameters of the clamping device are given in Table 2, which is determined in term of the joint variables, the first 3 elements represent the origin coordinates, the remaining 3 elements represent the orientation of the workpiece frame with respect to the work frame.

Table 2. Kinematic parameters of the clamping divice.

Links	x_i	y_i	z_i	α_i	β_i	η_i
0	x_0	y_0	z_0	*0*	*0*	*0*
B	x_d	y_d	z_d	*0*	*0*	*0*

Table 3 shows values of some major geometric and kinematic parameters of the robot. The table of mass, inetial tensor, the coordinates of the centers of mass, *etc.* are not presented here, because of its cumbersomeness.

Table 3. Kinematic parameters of the robot.

a_1	d_1	a_2	a_3	d_4	d_6	${}^6x_E$	${}^6y_E$	${}^6z_E$	${}^6\alpha_E$	${}^6\beta_E$	${}^6\eta_E$
300	514,5	700	280	1060,24	377	0	0	0	π	$\pi/2$	0

Table 4 shows the detail parameters of the workpiece and cutting process.

Table 4. Milling process parameters.

Material	h	S_v	v_c	n	L	D	B
C40	2,2	0,4	61,14	978	146,3	20	16

Units of the tables: Length-mm, force-Newton, depth of cut h-mm, n-rpm, feed rate S_v-mm/rev, velocity v_c-m/s.

All the calculations are performed for milling the assembly surface of the middle housing of the hydraulic pump with the parametes given in Table 4. The computation is carried out for a milling process following the tool path L which is a circle with radius of 0.09 m.

Figure 5 shows the form-shaping path or the tool path in the workpiece frame, the results of computation of the operational coordinates are shown in Figure 6. It can be seen that, the machining surface is a plane and the plane of the workpiece frame is coincident with the milling plane, therefore the operational coordinates along z_d axis and rotation about x_d and y_d axes are equal to zeros.

Figures 7 and 8 show the joint positions and joint velocities, respectively. Figure 9 shows the cutting force, compared between the average values of the cutting force with and without considering the vibration effects. Here, we neglected the moments acting about the x and y axes.

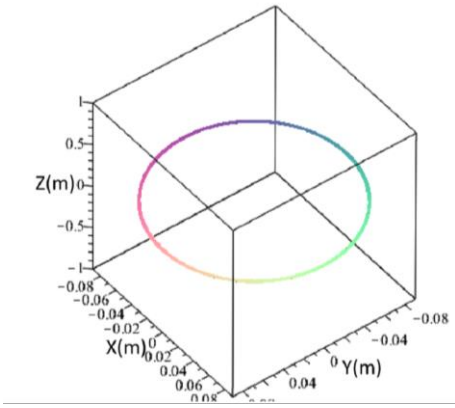

Figure 5. The form-shaping path.

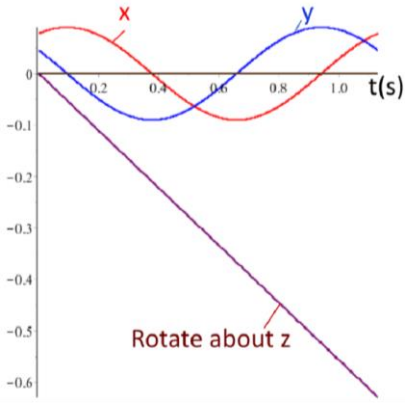

Figure 6. Operational space coordinates.

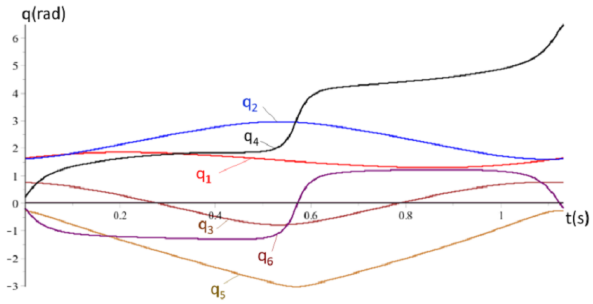

Figure 7. Joint coordinates.

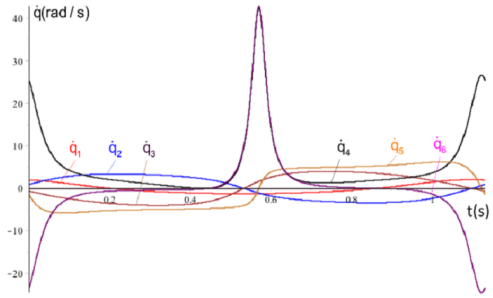

Figure 8. Joint velocities.

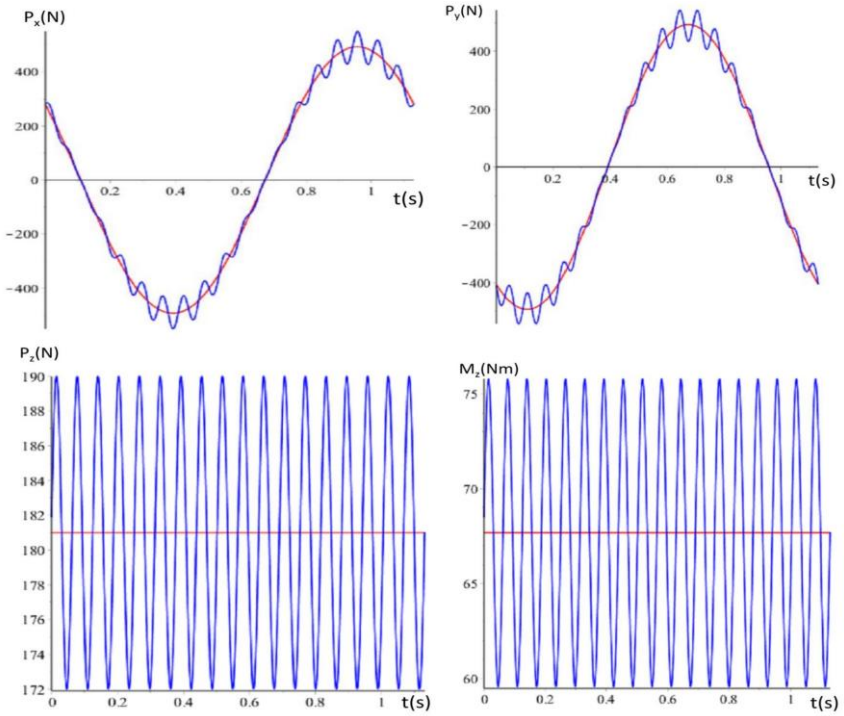

Figure 9. Cutting force values: the red lines - average values without vibration, the blue line-values with vibration.

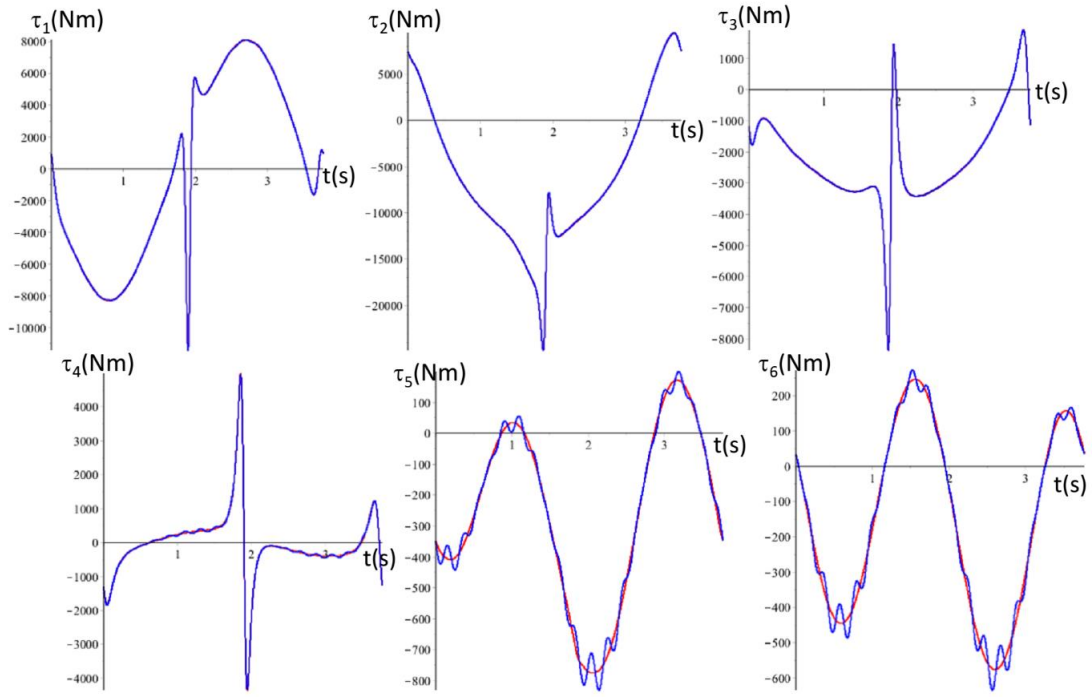

Figure 10. Driving forces: red-without vibration, blue-with vibration.

The results of inverse dynamic computation are given in Figure 10. The graphs on Figure 10 show the driving torques of the joints in the two cases with and without considering the deviations of the cutting force caused by vibrations.

5. CALIBRATION OF CUTTING FORCE

As presented above, computed cutting force values contain errors comparing to the actual values, this affects the control process base on the dynamic model. Fortunately, the sensors of the control system enable to measure the position, velocity, acceleration of the controled links of the robot. Depending on this approach, before we compute the inverse dynamic model to determine the driving forces, we carry out a step of cutting force calibration.

Suppose that the parameters of geometry, kinematics and dynamics of the differential equations of motion (21) are accurate. In controlling the robot process, the controller provides torque values; the sensors give information of robot motion.

The differential equations of motion in the form of (21) will become the form of (36) with taking into account the deviations of the cutting forces. The component ΔQ of equation (36) is the deviations of the general force corresponding to the deviations of the cutting forces. Rewrite (36) into (37), the right side of (37) is determined.

$$\Delta Q = U - \left[M(q)\ddot{q} + C(q,\dot{q}) + G(q) + Q\right] \tag{37}$$

Finally, we obtained (38):

$$\Delta R = J^{-1}\left\{U - \left[M(q)\ddot{q} + C(q,\dot{q}) + G(q) + Q\right]\right\} \tag{38}$$

Equation (38) enables to determine again cutting force values in a single computing step, this helps to modify driving torque values in robot control process.

It is easy to verify the algorithm of cutting force calibration. Assume that the cutting forces are calculated as the example in section 4, with average values, not taking into account the errors cause by vibrations. The sensors measure the motion as the case of taking into account vibration effects. Cutting force errors will be determined by using (38). Figure 11 shows calculated of the cutting force errors, which are caused by vibration effects, which are prented in section 4.

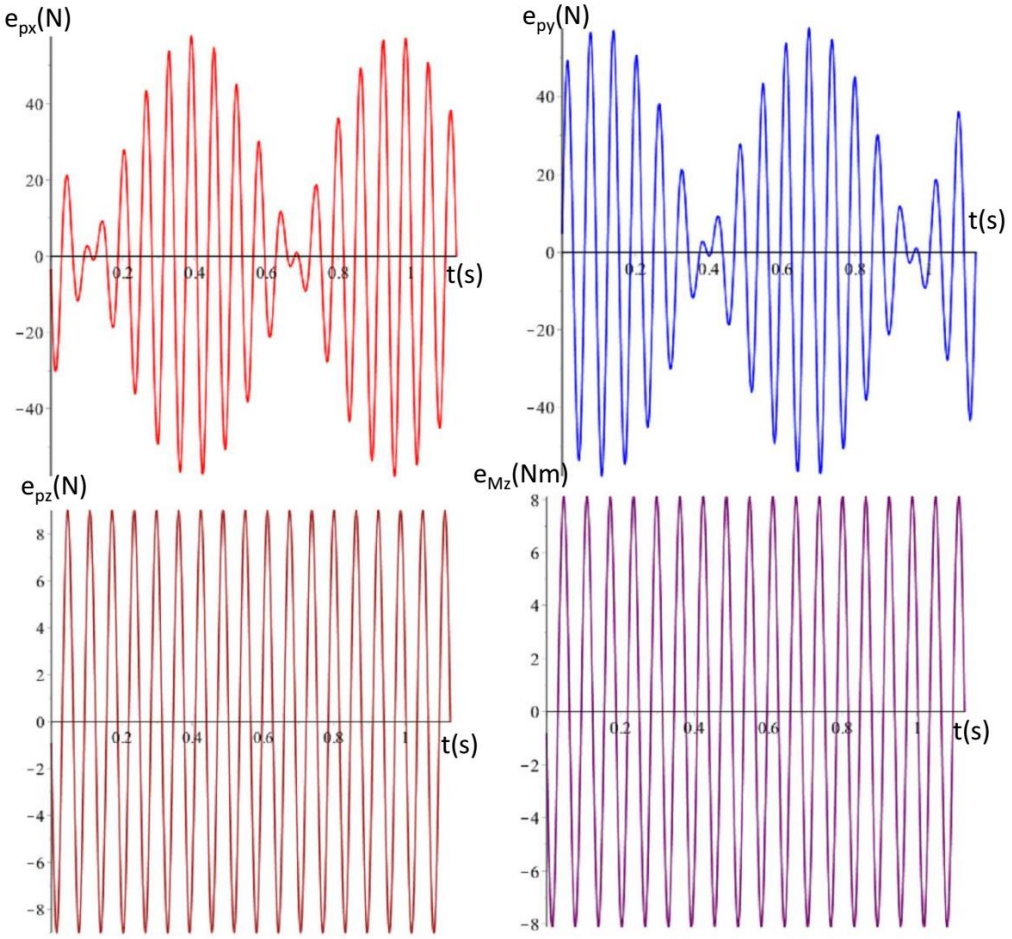

Figure 11. Cutting force errors.

6. CONCLUSIONS

The paper utilizes the method of the transformation coordinates and the homogeneous transformation matrices to derive and solve the kinematic and dynamic equations of the robot.

The proposed method of computing the cutting forces in the differential equations of the robot enables analyzing, computing the robot dynamics and driving torques taking into account the vibration factors that make cutting forces varying in machining processes.

The presented approach of determining and computing of calibrating cutting force values is convenient to use and helps to increase the accuracy of cutting force calculation as well as control robot motion base on its dynamic model.

The simulation results verified the validity of the proposed computing algorithms.

REFERENCES

1. Appleton E., Williams D. J. - Industrial robot applications, HALSTED PRESS, New York 1987, 229 pages.
2. Wei Ji, Lihui Wang - Industrial robotic Machining: A review, The International Journal of Advanced manufacturing Technology, September 2011, pp. 1-17.
3. John Pandremenos, Christos Doukas, Panagiotis Stavropoulos, George Chryssolouris - Machining with robots: a critical review, Proceedings of DET2011 7th International Conference on Digital Enterprise Technology, Athens, Greece, 28-30 September 2011.
4. Maciej Petko, Konrad Gac, Grzegorz Góra, Grzegorz Karpiel, Janusz Ochoński, Konrad Kobus - CNC system of the 5-axis hybrid robot for milling. Mechatronics **37** (2016) 89-99.
5. Iglesiasa I, Sebastiána M A, Aresc J E - Overview of the state of robotic machining: Current situation and future potential. ScienceDirect, Procedia Engineering **132** (2015) 911-917.
6. Maciej Petko, Grzegorz Karpiel, Konrad Gac, Grzegorz Góra, Konrad Kobus, Janusz Ochoński - Trajectory tracking controller of the hybrid robot for milling, Mechatronics **37** (2016) pp. 100-111.
7. Phan Bui Khoi, Ha Thanh Hai - Investigation of kinematics and motion planning for mechanical machining robots. Proceedings of the National Conference of Engineering Mechanics **2** (2015) 407-418 (in Vietnamese).
8. Phan Bui Khoi, Ha Thanh Hai - Robot dynamics in mechanical processing. Proceedings of the National Conference of Engineering Mechanics **2** (2015) pp. 419-427 (In Vietnamese).
9. Phan Bui Khoi, Ha Thanh Hai - Force analysis of a robot in machining process, Proceeding of National conference on machines and mechanisms, 2015, pp. 346-359.
10. Grzegorz Gołda, Adrian Kampa - Modelling of Cutting Force and Robot Load During Machining, Advanced Materials Research **1036** (2014) 715-720.
11. Lejun Cena and Shreyes N. Melkote - Effect of Robot Dynamics on the Machining Forces in Robotic Milling. ScienceDirect. 45th SME North American Manufacturing Research Conference, NAMRC 45, LA, USA 2017, pp. 486-496.
12. Adolfo Perrusquía, Wen Yu and Alberto Soria - Position/force control of robot manipulators using reinforcement learning. Industrial Robot: the international journal of robotics research and application **46** (2) (2019) 267-280.
13. Lacerda H. B. and Lima V. T. - Evaluation of Cutting Forces and Prediction of Chatter Vibrations in Milling, Journal of the Brazilian Society of Mechanical Sciences and Engineering **26** (1) (2004) 74-81.

14. Marco Leonesioa, Enrico Villagrossia, Manuel Beschia, Alberto Marinia, Giacomo Bianchia, Nicola Pedrocchia, Lorenzo Molinari Tosattia, Vladimir Grechishnikovb, Yuriy Ilyukhinb, Alexander Isaevb - Vibration analysis of robotic milling tasks, ScienceDirect, 11th CIRP Conference on Intelligent Computation in Manufacturing Engineering - CIRP ICME '17. 2018. pp. 262-267.
15. Guifeng Wang, Huiyue Dong, Yingjie Guo and Yinglin Ke - Dynamic cutting force modeling and experimental study of industrial robotic boring, The International Journal of Advanced Manufacturing Technology **86** (1-4) (2016) 179-190.
16. Banh Tien Long, Bui Ngoc Tuyen - Theory of surface formation and application in mechanical engineering, Vietnam Education Publisher, 2013, 244 pages (in Vietnamese).
17. Le Van Tham, Phan Bui Khoi, Bui Ngoc Tuyen, Cu Xuan Hung, Nguyen Duc Toan - Trajectory planning of robot, application for grinding the cutting blade of the curved-tip medical surgical scissor, Proceeding of the 2th National conference on Mechanics and Automation, Ha Noi, 2016. pp. 467-472 (in Vietnamese).
18. Phan Bui Khoi, Le Quang Huy, Nguyen Quoc Phu, Nguyen Viet Bach, Nguyen Dinh Man - Kinematic Modeling of the process of grinding turbine blades using robots, Proceeding of the 10th National conference on Mechanics, Hanoi, 8-9/12/2017, Vol. 1, Dynamics and Control-Mechanics of Machine, pp. 803-812 (in Vietnamese).
19. Phan Bui Khoi – Lecture of robotics, HUST 2009.
20. Altintas, Yusuf - Manufacturing automation: metal cutting mechanics, machine tool vibrations, and CNC design. Cambridge university press, 2012.
21. Adem, Khaled AM: Effects of machining system parameters and dynamics on quality of high-speed milling, PhD diss. University of Missouri-Columbia, 2013.